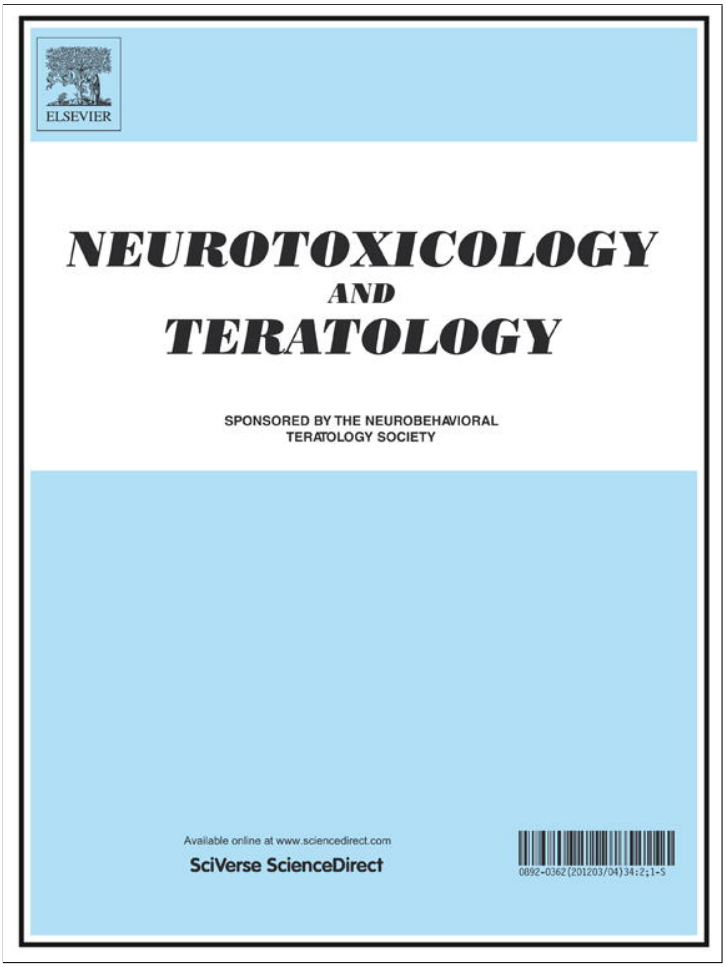

Neurotoxicology and Teratology 37 (2013) 57–62

Contents lists available at SciVerse ScienceDirect

Neurotoxicology and Teratology

journal homepage: www.elsevier.com/locate/neutera

Astrogliosis and HSP 70 activation in neonate rats' brain exposed to sodium metavanadate through lactation

Santiago Cuesta, Ramiro Proietto, Graciela Beatriz García *

Morphology Department, School of Biochemical and Pharmaceutical Sciences, National University of Rosario, Suipacha 531, 2000 Rosario, Santa Fe, Argentina

ARTICLE INFO

Article history:
Received 23 July 2012
Received in revised form 7 March 2013
Accepted 18 March 2013
Available online 2 April 2013

Keywords:
Vanadium
Neonates
Astrogliosis
Lipid peroxidation

ABSTRACT

The effect of sodium metavanadate ($NaVO_3$) exposure on lipid oxidative damage in the CNS of suckling rats was studied. Using histological markers of cellular injury, we also studied the morphological alterations of neurons and astroglial cells in different regions of neonate rats CNS after $NaVO_3$ exposure. Dams of treated litters were intraperitoneally injected with 3 mg $NaVO_3$/kg body weight/day during 12 days starting on post-natal day (PND) 10. On the 21st PND, four pups of each litter were sacrificed by decapitation and six brain areas were removed for lipid peroxidation assay by the thiobarbituric acid (TBA) reaction, the other four were transcardially perfused-fixed and their brains were removed and cut with a cryostat. Brain sections were processed for: NADPHd histochemistry and anti-HSP70, anti-GFAP and anti-S100 immunohistochemistry. The relative optical density of the NADPHd stained layers and of S100 (+) astrocytes and the GFAP (+) astrocyte surface area in Cer and Hc were measured. Although MDA levels, S100 immunostaining and NADPHd activity didn't show differences between experimental and control groups, both astrogliosis and HSP70 activation were detected in Cer, while only the former was detected in Hc of V-exposed pups.

1. Introduction

The general population is increasingly exposed to vanadium (V), mostly as a result of the increased utilization of V-containing petroleum fuels (Byczkowski and Kulkarni, 1996). V is usually found to be the most abundant trace metal in petroleum samples and can be found in concentrations reaching 1500 mg kg^{-1} depending on the source of the crude oil (Amorim et al., 2007). Furthermore, it was demonstrated that particulate matter (PM), a component of air pollution, contains high levels of nickel and V and that both metals could physically enter the central nervous system (CNS) through the olfactory mucosa (Calderon Garcidueñas et al., 2003; Maciejczyk and Chen, 2005). Natural sources (continental dust, volcanic eruptions, sea salt spray, and forest fires) also contribute to V particulate concentrations in the atmosphere (Fortoul et al., 2011). General population is not exposed to V as sodium metavanadate but regardless of the chemical form or the route of administration, at cellular level, vanadate (V) predominates due to neutral pH. Then vanadate (V) becomes reduced to vanadyl (IV) mostly by the intracellular glutathione and is subsequently bound to proteins (Evangelou, 2002).

V-induced developmental toxicity was reported in mice exposed during pregnancy, but it was limited to skeletal defects (Carlton et al., 1982; Paternain et al., 1990; Bosque et al., 1993; Sanchez et al., 1991). V is transferred from pregnant rats to their fetuses crossing the placental barrier and from nursing rats to their pups via the maternal milk (Edel and Sabbioni, 1989). Treatment of female rats with sodium metavanadate ($NaVO_3$) during gestation and lactation alters the development of the offspring (decreased body weight, body length and tail length) at 5, 10 and 20 mg/kg/day (Domingo et al., 1986). Exposure to V during the perinatal period (up to weaning) reduced the viability and body growth in the offspring when it was administered to dams through drinking water (Poggioli et al., 2001). In a previous work, we have shown that the administration of $NaVO_3$ to nursing rats resulted in CNS myelin deficit, delay in eye opening and decreased muscular strength and locomotion in suckling pups (Soazo and Garcia, 2007).

The majority of the toxic and molecular effects of V have been related to oxidative stress caused by free radical generation. V-induced lipoperoxidation and its effect on antioxidant enzymes in liver, kidney and lung were stated (Donaldson et al., 1985; Elfant and Keen, 1987; Younes and Strubelt, 1991; Russanov et al., 1994). Researchers have shown that graded doses of $NaVO_3$ induce remarkably high levels of lipid peroxides in discrete areas of the rat's brain and demonstrated that V initiated peroxidative reactions with loss of fatty acids, individual lipid profiles and proteins in different regions of the brain (Sasi et al., 1994). We have shown that intraperitoneal administration of $NaVO_3$ to adult rats resulted in changes in locomotor activity and specific myelin stainings (Garcia et al., 2004), as well as high lipid peroxidation levels, astrogliosis, heat shock protein expression (HSP70) and oxide nitric synthase (NOS) activation in hippocampus (Hc) and cerebellum (Cer) (Garcia et al., 2005). Reactive oxygen

* Corresponding author. Tel.: +54 341 480 4592/93x249; fax: +54 341 480 4598.
E-mail addresses: cuestasantiago@hotmail.com (S. Cuesta), proietto@hotmail.com.ar (R. Proietto), ggarcia@fbioyf.unr.edu.ar (G.B. García).

0892-0362/$ – see front matter © 2013 Elsevier Inc. All rights reserved.
http://dx.doi.org/10.1016/j.ntt.2013.03.002

species formation and alteration of the oxidative defense system in Hc and Cer, were also detected in adult rats (Cuesta et al., 2011).

Proteins like heat shock protein 70 (HSP70) play an important role in the development of adaptation to stress, increasing their synthesis in response to a cellular oxidative stress. Most of the HSPs have a molecular chaperone activity and participate in protein biogenesis and in the protection of cells from deleterious environmental stresses such as heat shock, acute ischemia, acute hypoxia, cooling and some chemicals (De Maio, 1999; Ohtsuka and Suzuki, 2000). Since normal brain cells have little detectable HSP70 mRNA or protein, HSP70 expression is a useful marker of cellular injury and may help to identify previously unrecognized areas of vulnerability in the nervous system after a neurotoxic injury (Rajdev and Sharp, 2000). Non heat shock proteins, like metallothionein and nitric oxide synthase (NOS), are also activated during oxidative stress. NOS is responsible for the calcium dependent synthesis of nitric oxide (NO). Three NOS isoenzymes are known, two constitutive: nNOS and eNOS (in brain and endothelium respectively), and one inducible iNOS (in several cell types). In the brain, nNOS is almost selectively localized in neurons and coincides with the distribution of nicotinamide adenine dinucleotide phosphate diaphorase (NADPHd) (Hope et al., 1991; Vincent and Kimura, 1992; Vincent, 1994). NO and the product derived from NO and superoxide anion radical reaction, peroxynitrite ($ONOO^-$), are considered reactive oxygen species (ROS) (Mates, 2000). As the detection of NOS activity through NADPHd reaction demonstrates potential NO production, it serves as a cellular marker of this very particular ROS.

Another cellular reaction to CNS damage is astrogliosis. Astrocytic response with an increase in glial fibrillary acidic protein (GFAP) is induced by many neurotoxicants (O'Callaghan, 1991, 1993). Thus, enhanced expression of GFAP appears as a marker of all types of brain injuries. S100 protein, a glial cell cytoplasmic protein, is also a reliable indicator of astrogliosis (Gomez et al., 1990; Jesse et al., 2009).

As we have found that $NaVO_3$ induces oxidative stress and lipid peroxidation in adult rats' Hc and Cer, we were interested in testing whether the lipid peroxidation observed in adults could also occur in developing rats. Moreover, using histological markers of cellular injury, we studied the morphological alterations of neurons and astroglial cells in different regions of lactating rats' CNS after $NaVO_3$ exposure.

2. Materials and methods

2.1. Chemicals

Polyclonal anti-GFAP (G 9269) and anti-S100 (S 2644) and monoclonal anti-HSP70 (clone BRM22-H5147) antibodies, anti rabbit IgG, rabbit peroxidase–antiperoxidase complex (PAP), anti mouse IgG, mouse PAP complex and diaminobenzidine hydrochloride (DAB) and all other chemicals were purchased from Sigma Chemical Co. (St. Louis, MO-USA).

2.2. Animals

Eight litters of newborn rats (Wistar origin), 1 day after birth, were used. Litters were reduced to eight animals (four males and four females if possible) to ensure good nutrition. The offspring, together with their mother, were housed in plastic breeding cages in a temperature-controlled nursery (22 ± 2 °C, relative humidity 40–60% and 12-h light/12-h dark cycle) with food and water ad lib. All the experimental protocols were performed according to the Guide to the Care and Use of Experimental Animals (Canadian Council on Animal Care) and according to the Regulation for the Care and Use of Laboratory Animals (Expedient 6109/012 E.C. Resolution 267/02) approved by the executive council of the School of Biochemistry and Pharmaceutical Sciences of Rosario—National University of Rosario.

2.3. Treatment

8 litters were randomly assigned to one of the following groups: V-treated group: consisted of offspring of 4 dams treated with $NaVO_3$. Since it was shown that in maternal milk V is transported in a bio-complex with lactoferrin which is a form of V available for the newborn during lactation (Edel and Sabbioni, 1989) in this group, dams were intraperitoneally (i.p.) injected with 3 mg/kg body weight (bw) of $NaVO_3$ [1.25 mg V/kg bw/day] in distilled water from the 10th to the 21st post natal day (PND). This dose of V was dictated by previous results, which indicated that the administration of similar amounts of $NaVO_3$ resulted in a delay in eye opening, decreased muscular strength and locomotion and decreased myelin staining in neonate rats (Soazo and Garcia, 2007). Control group: consisted of offspring of 4 dams that were injected (i.p.) with an equal volume (400 to 500 μl) of saline solution during the same period. Control and $NaVO_3$-exposed pups' body weight was recorded daily.

2.4. Biochemical determinations

2.4.1. MDA detection

Sixteen animals of each group (four pups per litter, two males and two females) were sacrificed by decapitation and selected brain areas (hypothalamus, prefrontal cortex, striatum, hippocampus, cerebellum and midbrain) were removed according to Heffner et al. (1980). The tissues were weighed using a high precision electronic balance and homogenized with cold distilled water. The homogenates were sonicated for fifteen seconds and then centrifuged for 4 min in an Eppendorf centrifuge (10,000 *g*) at 4 °C. An aliquot of the supernatant was used for protein determination by the Bradford method (Bradford, 1976) using bovine serum albumin as a standard. The results were expressed as mg of protein/g of tissue. Lipid peroxidation was determined by the thiobarbituric acid (TBA) reaction as follows: two volumes of TCA/TBA/HCl (15%:0.375%:0.25 N) for each volume of the homogenate were added and the mixture was incubated at 100 °C for 15 min. After centrifugation (10 min, 1000 *g*), absorbance was determined at 535 nm in a Beckman DU 640 spectrophotometer (Hall and Andrus, 2000). Malondialdehyde (MDA) concentration was obtained using the molar extinction coefficient. Results were expressed as nmol of MDA/mg of protein.

2.5. Histological studies

Four pups of each litter (selected as in 2.3.1) were i.p. anesthetized with 50 mg/kg sodium thiopental and transcardially perfused-fixed with 4% paraformaldehyde in a buffer phosphate 0.1 M (pH 7.4) solution. A brief wash with saline solution, 0.9% w/v NaCl, with 10 μl of 0.4 M $NaNO_2$ and 50 IU of heparin was passed through their circulatory system prior to fixation. Brains were kept in the same fixative solution for 2–4 h and immersed in 20% sucrose overnight or until they fell down. 40 μm-thick longitudinal brain sections were cut with a cryostat and kept at −20 °C cryoprotected with 30% sucrose in PBS.

2.5.1. NADPHd histochemistry

Since the histochemical detection of NADPHd-producing neurons is indicative of NOS activity in fixed tissues (Hope et al., 1991; Matsumoto et al., 1993), brain free floating sections were stained with the Nitro Blue Tetrazolium (NBT) modified method of Vincent and Kimura (1992). Two animals per litter were used. Control and treated brain sections were simultaneously incubated at 37 °C for 30 min in a 0.1 M phosphate buffer (pH 7.4) solution containing: 1 mg/ml β-NADPH, 0.1 mg/ml NBT and 0.3% Triton X-100. To stop the reaction, sections were transferred to phosphate buffer and rinsed with distilled water. Then, they were mounted on gelatinized standard glass slides, coverslipped and examined using a light microscope.

2.5.2. Immunohistochemical procedures

Brain floating sections from two exposed and control pups per litter were simultaneously processed. The same protocol was used for each step of immunohistochemical staining according to Sternberger's peroxidase–antiperoxidase (PAP) technique (Sternberger et al., 1970) using polyclonal anti-GFAP antibody (developed in rabbit) 1:8000 and anti-S100 1:8000 and monoclonal anti-HSP70 antibody (developed in mouse) 1:2000 as primary antibodies. Development of peroxidase activity was performed with DAB/nickel ammonium sulfate in acetate buffer (0.1 M, pH 6) at room temperature for GFAP and S100 and with DAB in phosphate buffer (0.1 M, pH 7.4) at room temperature for HSP70. Two to three sections of each animal were mounted on gelatinized standard glass slides for light microscopy study.

2.6. Computerized image analysis

The relative optical density (ROD) of the NADPHd stained cerebellar molecular and granular layers and of S100 immunoreactive (IR) astrocytes and the GFAP-(IR) astrocyte surface area in Cer and Hc were measured using a NIH imaging analysis system. Images were obtained through an Olympus D-560 zoom digital camera (Olympus America Inc., New York, USA) attached to an Olympus BX40 microscope (Olympus Optical Co., Ltd. Japan).

The mean gray value of the NBT stained cerebellar molecular and granular layers was measured using a rectangular area of interest (AOI). This AOI was located 4–5 times in each layer and the mean gray values were taken. Relative optical density (ROD) was obtained after a transformation of mean gray values into ROD using the formula: ROD = log (256/mean gray). The ROD value was chosen to evaluate the intensity of NBT staining. ROD was calculated and averaged within the experimental group in each animal per layer.

In order to evaluate astrogliosis in Hc and Cer, images from anatomically matched regions of each experimental group were used. After image segmentation, the cross sectional area of all GFAP-IR astrocytes was measured. The average for each experimental group represents the mean surface area of GFAP-IR cells present per individual. In S100 immunocytochemistry, ROD of all S100-IR astrocytes was measured after image segmentation.

2.7. Statistical analysis

Statistical analyses were carried out using the Instat/PC program. All data are presented as litters' means ± SD. Litters' means were tested by the Student's *t* test. Data of each litter were previously evaluated by ANOVA looking for interaction between sexes. In all cases, the significance level was considered to be $p < 0.05$.

3. Results

3.1. Maternal data

At the end of $NaVO_3$ administration, body weight gain in treated dams (−6.25 ± 2.87 g) was significantly lower ($p = 0.04$) compared to control dams (2.00 ± 5.75 g) without any other sign of illness. This suppression in body weight increment is typical of V intoxication and could be related to a reduced food intake (Wang et al., 2001).

3.2. Body and brain weight

Before and during dams' treatment, newborn mortality was not observed. At the end of $NaVO_3$ administration, there were no significant differences in body ($p = 0.06$) and brain ($p = 0.10$) weight between control and $NaVO_3$-exposed pups of both sexes (Table 1). Signs of overall toxicity such as pallor, asphyxia, lethargy or diarrhea were not observed.

3.3. MDA detection

No differences in the final concentrations of TBA-reactive material were observed in any brain area homogenates of $NaVO_3$-exposed pups when compared to the corresponding control homogenate. As there were no differences between sexes, data of the four pups were averaged in order to have the litter's mean. Data expressed as nmol of MDA/mg protein are shown in Table 2.

3.4. Microscopic studies

3.4.1. NADPHd histochemistry

Histochemical detection of NADPHd activity was assumed as a measure of NOS activity in brain sections. Computerized image analysis (CIA) of NBT staining could be interpreted as a specific augmentation of NOS expression in neurons. However, in Cer ($p = 0.08$), cortex ($p = 0.16$) and striatum ($p = 0.23$) of $NaVO_3$-exposed pups, NBT staining was not statistically different to control ones (data not shown).

3.4.2. HSP70 immunohistochemistry

In the Cer, HSP70 immunoreactivity was detected in molecular and granular layers, and Purkinje cells also became immunostained after $NaVO_3$ exposition (Fig. 1). In the Hc, HSP70 immunoreactivity was diffusely distributed in all layers of control and $NaVO_3$-exposed pups (data not shown).

3.4.3. GFAP immunohistochemistry

GFAP immunostaining specifically labels the intermediate filaments of the astroglial cytoskeleton, allowing the study of astrocyte morphology. GFAP immunostaining shows the cell body of astrocytes as well as their numerous processes. GFAP-IR astrocytes in cerebellum, mainly those in the white matter, were markedly larger in the $NaVO_3$-exposed animals (Fig. 2A). CIA data confirmed these observations: average GFAP-IR astrocytic surface area was 36.30 ± 3.0 μm^2 in $NaVO_3$-exposed pups while it was 30.50 ± 2.8 μm^2 for control pups, $p = 0.03$ (Fig. 2B). In the Hc, GFAP-IR cells appeared more densely grouped in the hilus and in the subiculum in both experimental groups (Fig. 3A and B). In the hippocampal hilus of $NaVO_3$--exposed pups, astrocytes presented enlarged thick processes and increased soma size (Fig. 3C), the average GFAP-IR astrocytic surface area was 33.79 ± 2.60 μm^2 in $NaVO_3$-exposed pups, while in the control group it was 25.53 ± 1.39 μm^2, $p = 0.010$ (Fig. 3D). However, no differences between $NaVO_3$-exposed and control pups in GFAP-IR astrocytic surface area in hippocampal subiculum ($p = 0.09$) were detected (data not shown).

3.4.4. S100 immunohistochemistry

S100 proteins appeared to be confined to the cytosol of both normal and reactive astrocytes. S100 immunostaining labeled the astrocyte cell body and some cytoplasmic projections. S100 immunostaining was observed in the astroglial cells of every analyzed brain region in control and treated groups although, the immunostaining intensity was similar both in control and $NaVO_3$-exposed pups in Cer ($p = 0.30$) and Hc [hilus ($p = 0.69$) and subiculum ($p = 0.28$)] (data not shown).

Table 1
Body and brain weight in vanadium exposed pups.

Groups	Body weight	Brain weight
Control	46.30 ± 9.12	1.28 ± 0.03
3 mg $NaVO_3$/kg bw/day	39.23 ± 3.84	1.21 ± 0.05

The weights are expressed in grams. Each value is the mean ± SD of 4 litters.

Table 2
Concentrations of MDA/mg protein in various brain areas.

Brain regions	Control	$NaVO_3$-exposed	*p*
Hypothalamus	1.18 ± 0.39	1.49 ± 0.78	0.52
Prefrontal cortex	2.06 ± 0.84	1.85 ± 0.62	0.72
Striatum	1.50 ± 0.33	1.43 ± 0.49	0.85
Hippocampus	1.91 ± 0.89	1.66 ± 0.76	0.64
Midbrain	1.18 ± 0.19	1.14 ± 0.17	0.30
Cerebellum	1.67 ± 0.26	1.70 ± 0.47	0.89

Results are expressed as nmol MDA/mg protein. Each value is the mean ± SD of 4 litters.

4. Discussion

Although MDA levels, S100 immunostaining and NADPHd activity didn't show differences between experimental and control groups, both astrogliosis and HSP70 activation were detected in Cer, while only the former was detected in the hippocampal hilus of V-exposed pups.

Both normally and after brain injury, astrocytes support neurons by providing antioxidant protection, substrates for neuronal metabolism, and glutamate clearance (Barreto et al., 2011). Reactive astrogliosis occurs in response to CNS injury and disease, including subtle perturbations. In the present study a mild to moderate reactive astrogliosis in $NaVO_3$-exposed pups was observed. Moderate astrogliosis comprises variable changes in molecular expression and functional activity together with variable degrees of cellular hypertrophy with preservation of the individual nonoverlapping domains of reactive astrocytes (Sofroniew, 2009). Reactive astrocyte changes vary with the nature and severity of the insult and are regulated by specific signaling events. Molecular mediators of reactive astrogliosis can be released by any cell type in CNS tissue. Moreover ROS and NO molecules are able to trigger aspects of reactive astrogliosis (Swanson et al., 2004). Astrocytes changes, during reactive astrogliosis, alter its activities both through gain and loss of

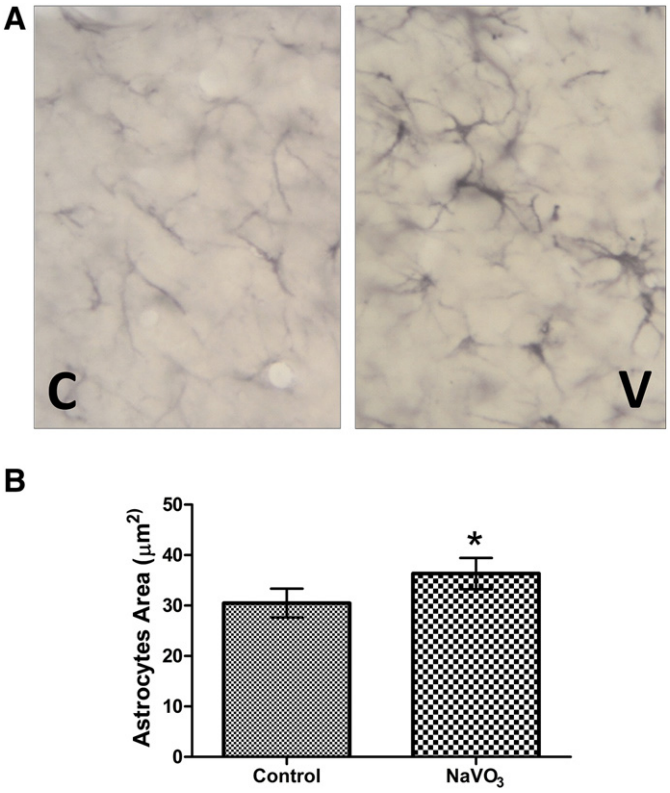

Fig. 2. A: GFAP immunostained cerebellum of control (C) and $NaVO_3$-exposed (V) pups. GFAP-IR astrocytes localized in cerebellum white matter are markedly large and with more tortuous cytoplasmic processes in $NaVO_3$-exposed (V) pups. Primary magnification 400×. B: GFAP-IR astrocytic surface area in cerebellum. Each bar shows the mean ± SD of the GFAP-IR astrocytic surface area of control and $NaVO_3$-exposed pups (n = 4 for each group). *$p < 0.05$ with reference to control.

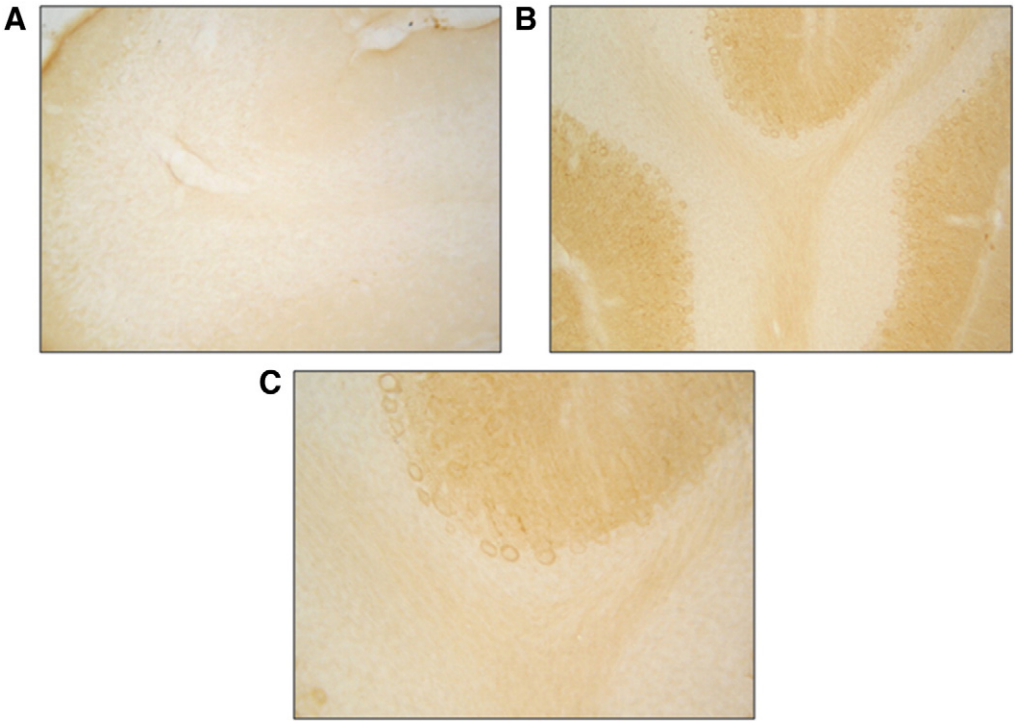

Fig. 1. HSP70 immunostained cerebellum of control (A) and $NaVO_3$-exposed (B) pups, primary magnification: 100×. Molecular and Purkinge cell layers became stained after $NaVO_3$ exposition (C), primary magnification: 200×.

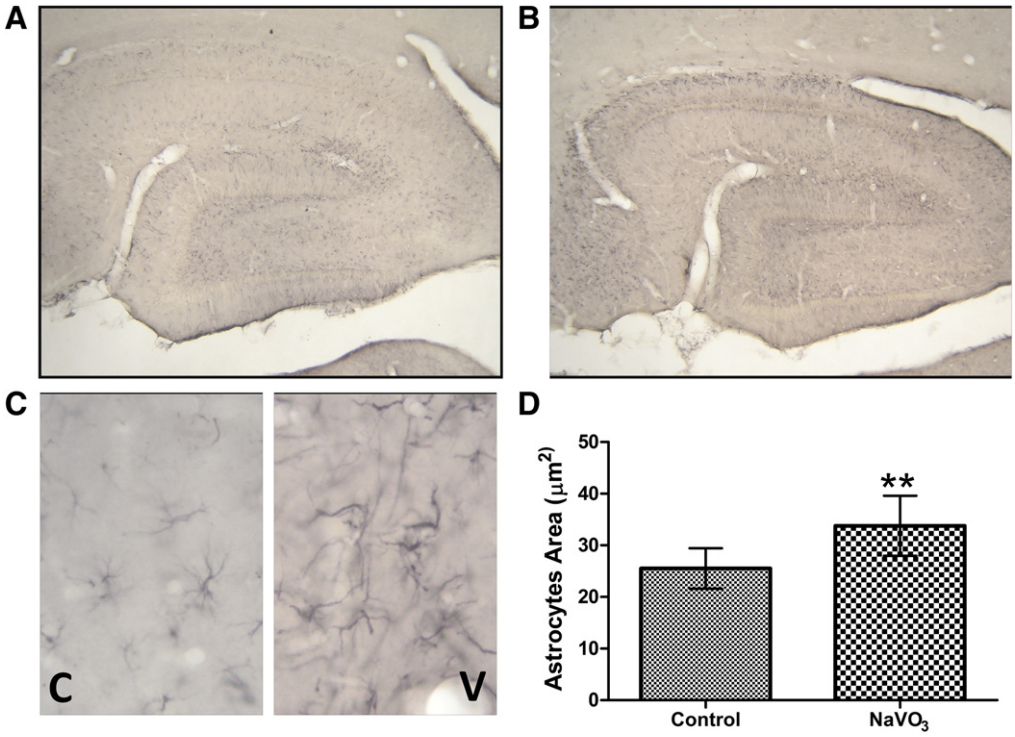

Fig. 3. GFAP immunostained hippocampus of control (A) and $NaVO_3$-exposed (B) pups, primary magnification: 40×. C: GFAP immunostained astrocytes of control (C) and $NaVO_3$-exposed (V) pups' hippocampal hilus. Astrocytes presented enlarged thick processes and increased soma size in the $NaVO_3$-exposed pups. Primary magnification 400×. D: GFAP-IR astrocytic surface area in the hippocampal hilus. Each bar shows the mean ± SD of the GFAP-IR astrocytic surface area of control and $NaVO_3$-exposed pups (n = 4 for each group). $^{**}p < 0.01$ with reference to control.

functions that can impact both beneficially and detrimentally on surrounding neural and non-neural cells. In vitro and in vivo studies show that astrocytes under different conditions can alter the expression of molecules involved in oxidative stress (NO, NOS, SOD and GSH) (Chen et al., 2001; Hamby et al., 2006) and that reactive astrocytes can protect CNS cells and tissue in various ways, including protection from oxidative stress via glutathione production (Shih et al., 2003; Swanson et al., 2004; Vargas et al., 2008; Sofroniew, 2009). In a previous work, in adult rats exposed to the same dose of $NaVO_3$ for 5 days, we have found lipid peroxidation, astrogliosis, NADPHd activation and decreased levels in the ratio GSH/GSSG in Hc and Cer (Garcia et al., 2004, 2005; Cuesta et al., 2011). However, $NaVO_3$ exposure – in the dose and period used in the present work – does not induce lipid peroxidation, but astrogliosis and HSP70 activation were detected in suckling rats. Increased activities of antioxidant enzymes or enhanced glutathione content in reactive astrocytes could explain these results.

In the present work we assumed that with our dosage V was present in the milk of $NaVO_3$ treated dams. However, since V is poorly (only about 10%) absorbed from the suckling pups' gastrointestinal tract (Mukherjee et al., 2004), it could be insufficient to induce lipoperoxidation in their brains. Furthermore, HSP70 expression is closely linked to redox changes and higher activities of antioxidant enzymes have been positively correlated with increased HSP70 synthesis in astroglial cell cultures (Barger and Van Eldik, 1992). HSP70 by its traditional chaperoning role is involved in conferring cytoprotective effects to the cellular proteins from oxidative milieu. Moreover, HSP70 and other heat shock proteins can also serve as cytoplasmic "antioxidants" by protecting the sensitive sites of target proteins (Papp et al., 2003).

On the other hand, S100 protein may play a dual role in the regulation of cell function being beneficial to cells at low doses but detrimental at high doses (Hu et al., 1996). In studies using a neuronal and astroglial co-culture, a high concentration of S100 upregulated NO release from the astroglia, which was shown to be neurotoxic (Hu and Ferreia, 1997; Nawashiro et al., 2000). In a previous work in adult rats, astrocytes' S-100 intensity, NBT staining and MDA levels were increased in the Cer and the Hc in $NaVO_3$-exposed animals (Garcia et al., 2004, 2005). However, $NaVO_3$ exposure – in the dose and period used in the present work – does not increase S100 intracellular levels as well as NADPHd activity in $NaVO_3$-exposed pups. S100β has important autocrine and paracrine, neurotrophic and gliotrophic actions (Mrak et al., 1995). S100β acts on neurons (paracrine effects) to induce increased cytoplasmic free calcium levels, to stimulate neurite outgrowth, and to promote neuronal survival and on astrocytes (autocrine effects) to increase intracellular free calcium levels and to promote astrocytic proliferation and hypertrophy (Barger and Van Eldik, 1992). In addition to these functions in mature brain, S100β also has important neurotrophic and gliotrophic roles during fetal development (Bhattacharyya et al., 1992; Sarnat, 1992).

In $NaVO_3$ exposed pups, a mild to moderate astrogliosis was detected but without increase in S100 protein synthesis. This fact could be temporary because, in the one hand, S100 synthesis could not have been enhanced yet; on the other hand, the absence of an S100 increase could also be due to its release into the intercellular space to exert its paracrine and/or autocrine effects.

In the present work, we found that dams' exposure to V during lactation induced astrogliosis and HSP70 activation in suckling pups. These results, together with previous ones (Soazo and Garcia, 2007), are indicating that V impairs the physical and neural development of the offspring. This developmental neurotoxicity may be manifested in various ways because it involves alterations in dam and offspring behavior, neurohistology and neurochemistry and should receive additional investigation based on the findings of this report.

Conflict of interest

Nothing declared.

Acknowledgments

The authors would like to thank Alejandra Martínez for technical assistance and Lucía Ruiz for her assistance in the correction of this paper.

Appendix A. Supplementary data

Supplementary data to this article can be found online at http://dx.doi.org/10.1016/j.ntt.2013.03.002.

References

Amorim FAC, Welz B, Costa ACS, Lepri FG, Vale M, Goreti R, Ferreira SLC. Determination of vanadium in petroleum and petroleum products using atomic spectrometric techniques. Talanta 2007;72:349–59.
Barger SW, Van Eldik LJ. S100β stimulates calcium fluxes in glial, and neuronal cells. J Biol Chem 1992;267:9689–94.
Barreto GE, Gonzalez J, Torres Y, Morales L. Astrocytic-neuronal crosstalk: implications for neuroprotection from brain injury. Neurosci Res 2011;71:107–13.
Bhattacharyya A, Oppenheim RW, Prevette D, Moore BW, Brackenbury R, Ratner N. S100 is present in developing chicken neurons, and Schwann cells, and promotes neuron survival in vivo. J Neurobiol 1992;23:451–66.
Bosque MA, Domingo JL, Llobet JM, Corbella J. Variability in the embryotoxicity and fetotoxicity of vanadate with the day of exposure. Vet Hum Toxicol 1993;35:1–3.
Bradford M. A rapid and sensitive method for the quantification of microgram quantities of protein utilising the principle of protein–dye binding. Anal Biochem 1976;72:248–54.
Byczkowski JZ, Kulkarni AP. Pro-oxidant biological effects of inorganic component of petroleum: vanadium and oxidative stress. (Report no. A647063). www.stormingmedia.us1996.
Calderon Garcidueñas L, Maronpont RR, Torres-Jardon R, Henriquez-Roldan C, Schoonhoven R, Acuña-Ayala H, Villarreal-Calderón A, Nakamura J, Reshan F, Reed W, Azzarelli B, Swenberg J. DNA damage in nasal and brain tissues of canines exposed to air-pollutants is associated with evidence of chronic brain inflammation and neurodegeneration. Toxicol Pathol 2003;31:524–38.
Carlton BD, Beneke MB, Fisher GL. Assessment of teratogenicity of ammonium vanadate using Syrian golden hamsters. Environ Res 1982;29:256–62.
Chen Y, Vartiainen NE, Ying W, Chan PH, Koistinaho J, Swanson RA. Astrocytes protect neurons from nitric oxide toxicity by a glutathione-dependent mechanism. J Neurochem 2001;77:1601–10.
Cuesta S, Francés D, García GB. ROS formation and antioxidant status in brain areas of rats exposed to sodium metavanadate. Neurotoxicol Teratol 2011;33:297–302.
De Maio A. Heat shock proteins: facts, thoughts and dreams. Shock 1999;11(1):1-12.
Domingo JL, Paternain JL, Llobet JM, Corbella J. Effects of vanadium on reproduction, gestation, parturition and lactation in rats upon oral administration. Life Sci 1986;39:819–24.
Donaldson J, Hemming R, La Bella F. Vanadium exposure enhances lipid peroxidation in the kidney of rats and mice. Can J Physiol Pharmacol 1985;63:196–9.
Edel J, Sabbioni E. Vanadium transport across placenta and milk of rats to the fetus and newborn. Biol Trace Elem Res 1989;22(3):265–75.
Elfant M, Keen CL. Sodium vanadate toxicity in adult and developing rats. Role of peroxidative damage. Biol Trace Elem Res 1987;14:193–207.
Evangelou AM. Vanadium in cancer treatment. Crit Rev Oncol Hematol 2002;42:249–65.
Fortoul TI, Rodriguez-Lara V, Gonzalez-Villalva A, Rojas-Lemus M, Cano-Gutierrez G, Ustarroz-Cano M, Colin-Barenque L, Montaño LF, García-Pelez I, Bizarro-Nevares P, Lopez-Valdez N, Falcon-Rodriguez CI, Jimenez-Martínez RS, Ruiz-Guerrero ML, Lopez-Zepeda LS, Morales-Rivero A, Muñiz-Rivera-Cambas A. Vanadium inhalation in a mouse model for the understanding of air-suspended particle systemic repercussion. J Biomed Biotechnol 2011;2011:1-11.
Garcia GB, Quiroga A, Strütz N, Martinez A, Biancardi ME. Morphological alterations of central nervous system (CNS) myelin in vanadium (V) exposed adult rats. Drug Chem Toxicol 2004;27:1-13.
Garcia GB, Biancardi ME, Quiroga AD. Vanadium (v)-induced neurotoxicity in the rat central nervous system: a histo-immunohistochemical study. Drug Chem Toxicol 2005;28:329–44.
Gomez L, Brusco A, Loidl C, Pecci Saavedra J. Ultrastructural localization of S 100 protein in reactive astrocytes. Commun Biol 1990;9(2):103–10.
Hall E, Andrus K. Measurement of oxygen radicals and lipid peroxidation in neural tissues. In: Gerfen C, Holmes A, Rogawsky M, Sibley D, Skolnick P, Wray S, editors. Current protocols in neuroscience. John Wiley and Sons; 2000.
Hamby ME, Hewett JA, Hewett SJ. TGF-b1 potentiates astrocytic nitric oxide production by expanding the population of astrocytes that express NOS-2. Glia 2006;54:566–77.
Heffner TG, Hartman JA, Seiden LS. A rapid method for the regional dissection of the rat brain. Pharmacol Biochem Behav 1980;13(3):453–6.
Hope BT, Michael GJ, Knigge KM, Vincent SR. Neuronal NADPH-diaphorase is a nitric oxide synthase. Proc Natl Acad Sci U S A 1991;88:2811–4.
Hu J, Ferreia A. S100β induces neuronal cell death through nitric oxide release from astrocytes. J Neurochem 1997;69:2294–301.
Hu J, Castets F, Guevana LJ. S100β stimulates inducible nitric oxide synthase activity and mRNA levels in rat cortical astrocytes. J Biol Chem 1996;271:2543–7.
Jesse S, Steinacker P, Cepek L, von Arnim CA, Tumani H, Lehnert S, Kretzschmar HA, Baier M, Otto M. Glial fibrillary acidic protein and protein S-100B: different concentration pattern of glial proteins in cerebrospinal fluid of patients with Alzheimer's disease and Creutzfeldt–Jakob disease. J Alzheimers Dis 2009;17(3):541–51.
Maciejczyk P, Chen LC. Effects of subchronic exposures to concentrated ambient particles (CAPs) in mice, VIII, source-related daily variations in in vitro responses to CAPs. Inhal Toxicol 2005;17:243–53.
Mates M. Effects of antioxidant enzymes in the molecular control of reactive oxygen species toxicology. Toxicology 2000;153:83-104.
Matsumoto T, Nakane M, Pollock JS, Kuk JE, Forstermann U. A correlation between soluble brain nitric oxide synthase and NADPH-diaphorase activity is only seen after exposure of the tissue to fixative. Neurosci Lett 1993;155:61–4.
Mrak RE, Sheng JG, Griffin WST. Glial cytokines in Alzheimer's disease: review and pathogenic implications. Hum Pathol 1995;26:816–23.
Mukherjee B, Patra B, Mahapatra S, Banerjee P, Tiwari A, Chatterjee M. Vanadium an element of atypical biological significance. Toxicol Lett 2004;150:135–43.
Nawashiro H, Brenner M, Fukui S, Shima K, Hallenbeck MJ. High susceptibility to cerebral ischemia in GFAP-null mice. J Cereb Blood Flow Metab 2000;20:1040–4.
O'Callaghan JP. The use of glial fibrillary acidic protein in first-tier assessments of neurotoxicity. J Am Coll Toxicol 1991;10:19–26.
O'Callaghan JP. Quantitative features of reactive gliosis following toxicant-induced damage of the CNS. In: Johannessen JN, editor. Markers of neuronal injury and degeneration, 679. New York: The New York Academy of Science; 1993. p. 195–210.
Ohtsuka K, Suzuki T. Roles of molecular chaperones in the nervous system. Brain Res Bull 2000;53(2):141–6.
Papp E, Nardai G, Soti C, Csermely P. Molecular chaperones, stress proteins and redox homeostasis. Biofactors 2003;17:249–57.
Paternain JL, Domingo JL, Gomez M, Ortega A, Corbella J. Developmental toxicity of vanadium in mice after oral administration. J Appl Toxicol 1990;10:181–6.
Poggioli R, Arletti R, Bertolini A, Frigeri C, Benelli A. Behavioral and developmental outcomes of prenatal and postnatal vanadium exposure in the rat. Pharmacol Res 2001;43(4):341–7.
Rajdev S, Sharp FR. Stress proteins as molecular markers of neurotoxicity. Toxicol Pathol 2000;28(1):105–12.
Russanov E, Zaporowska H, Ivancheva E, Kirkova M, Konstantinova S. Lipid peroxidation and antioxidant enzymes in vanadate-treated rats. Comp Biochem Physiol 1994;307C:415–21.
Sanchez DJ, Ortega A, Domingo JL, Corbella J. Developmental toxicity evaluation of orthovanadate in the mouse. Biol Trace Elem Res 1991;30:219–26.
Sarnat HB. Regional differentiation of the human fetal ependyma: immunocytochemical markers. J Neuropathol Exp Neurol 1992;51:58–75.
Sasi MM, Haider SS, el-Fakhri M, Ghwarsha KM. Microchromatographic analysis of lipids, protein, and occurrence of lipid peroxidation in various brain areas of vanadium exposed rats: a possible mechanism of vanadium neurotoxicity. Neurotoxicology 1994;15:413–20.
Shih AY, Johnson DA, Wong G, Kraft AD, Jiang L, Erb H, Johnson JA, Murphy TH. Coordinate regulation of glutathione biosynthesis and release by Nrf2-expressing glia potently protects neurons from oxidative stress. J Neurosci 2003;23:3394–406.
Soazo M, Garcia GB. Vanadium exposure through lactation produces behavioural alterations and CNS myelin deficit in neonatal rats. Neurotoxicol Teratol 2007;29(4):503–10.
Sofroniew MV. Molecular dissection of reactive astrogliosis and glial scar formation. Trends Neurosci 2009;32(12):638–47.
Sternberger LA, Hardy PH, Cuculis JJ, Mayer HG. The unlabeled antibody enzyme method of immunohistochemistry. Preparation and properties of soluble antigen–antibody complex (horseradish peroxidase–antihorseradish peroxidase) and its use in identification of spirochetes. J Histochem Cytochem 1970;28:315–33.
Swanson RA, Ying W, Kauppinen TM. Astrocyte influences on ischemic neuronal death. Curr Mol Med 2004;4:193–205.
Vargas MR, Johnson DA, Sirkis DW, Messing A, Johnson JA. Nrf2 activation in astrocytes protects against neurodegeneration in mouse models of familial amyotrophic lateral sclerosis. J Neurosci 2008;28:13574–81.
Vincent SR. Nitric oxide: a radical neurotransmitter in the central nervous system. Prog Neurobiol 1994;42:129–60.
Vincent SR, Kimura H. Histochemical mapping of nitric oxide synthase in the rat brain. Neuroscience 1992;46:755–84.
Wang J, Yuen VG, Mc Neill JH. Effect of vanadium on insulin sensitivity and appetite. Metabolism 2001;50:667–73.
Younes M, Strubelt O. Vanadate-induced toxicity towards isolated perfused rat livers: the role of lipid peroxidation. Toxicology 1991;66:63–74.